Fig. S1

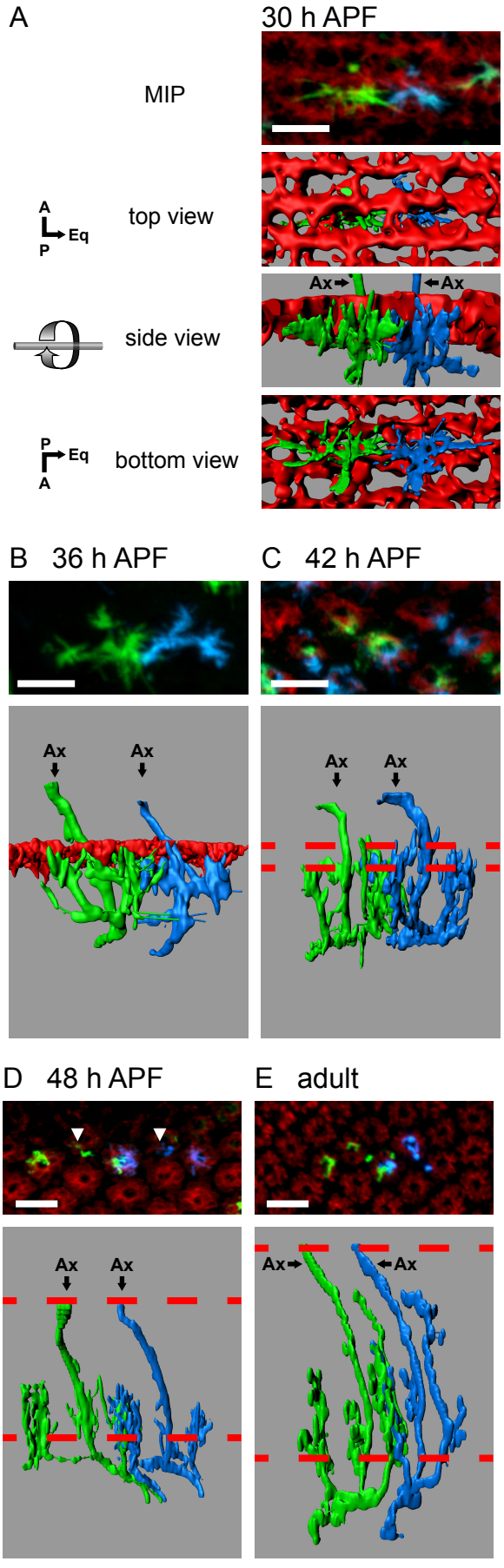
A
30 h APF
MIP
top view
A
Eq
P
side view
Ax
Ax
bottom view
P
Eq
A
B 36 h APF
C 42 h APF
Ax
Ax
Ax
Ax
D 48 h APF
E adult
Ax
Ax
Ax
Ax

Fig. S2

A Dscam2A isoform reporter

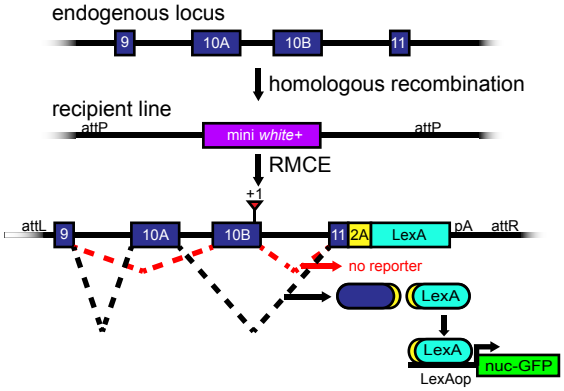

B Dscam2 lamina neuron expression

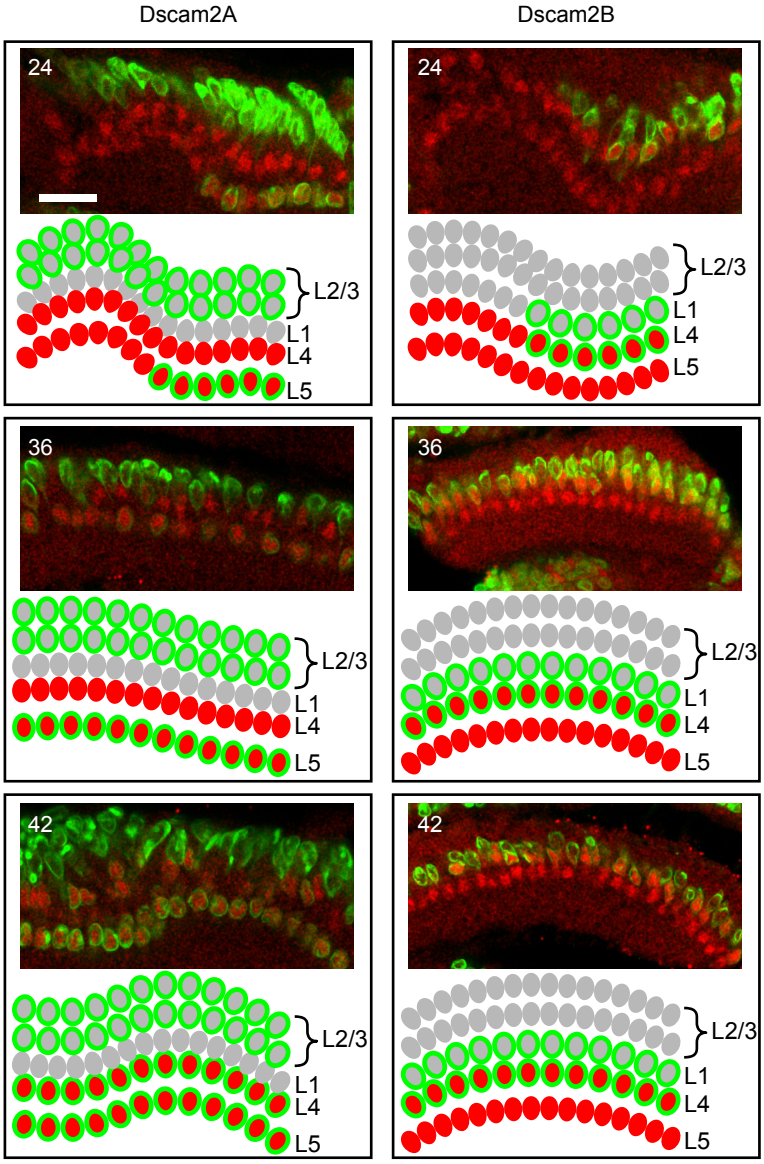

C Dscam2B R cell expression

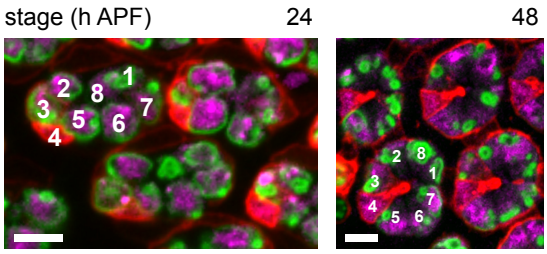

D Dscam2 protein tag

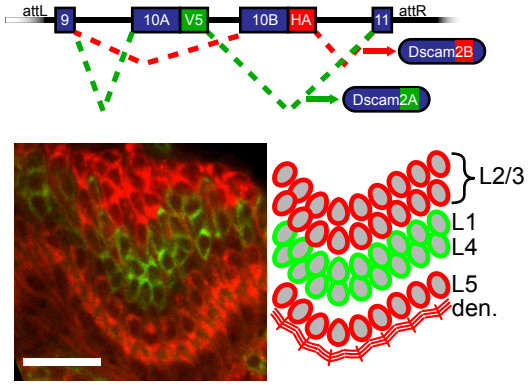

E MARCM: Dscam2 isoform alleles at 24 h APF

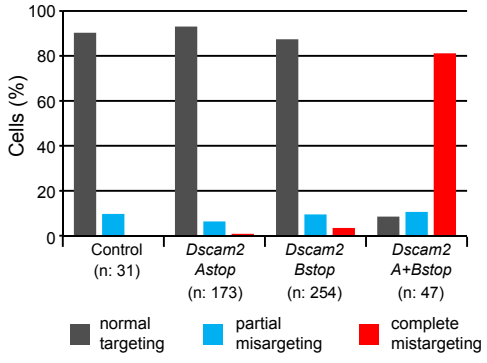

F Dscam2A expression in *Dscam2Bstop* background

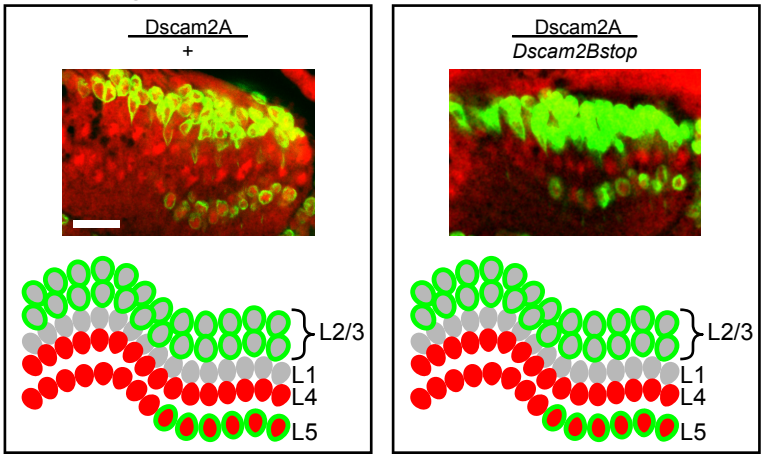

Fig. S3

A

Reverse MARCM

L4 - Lamina Neuron interactions

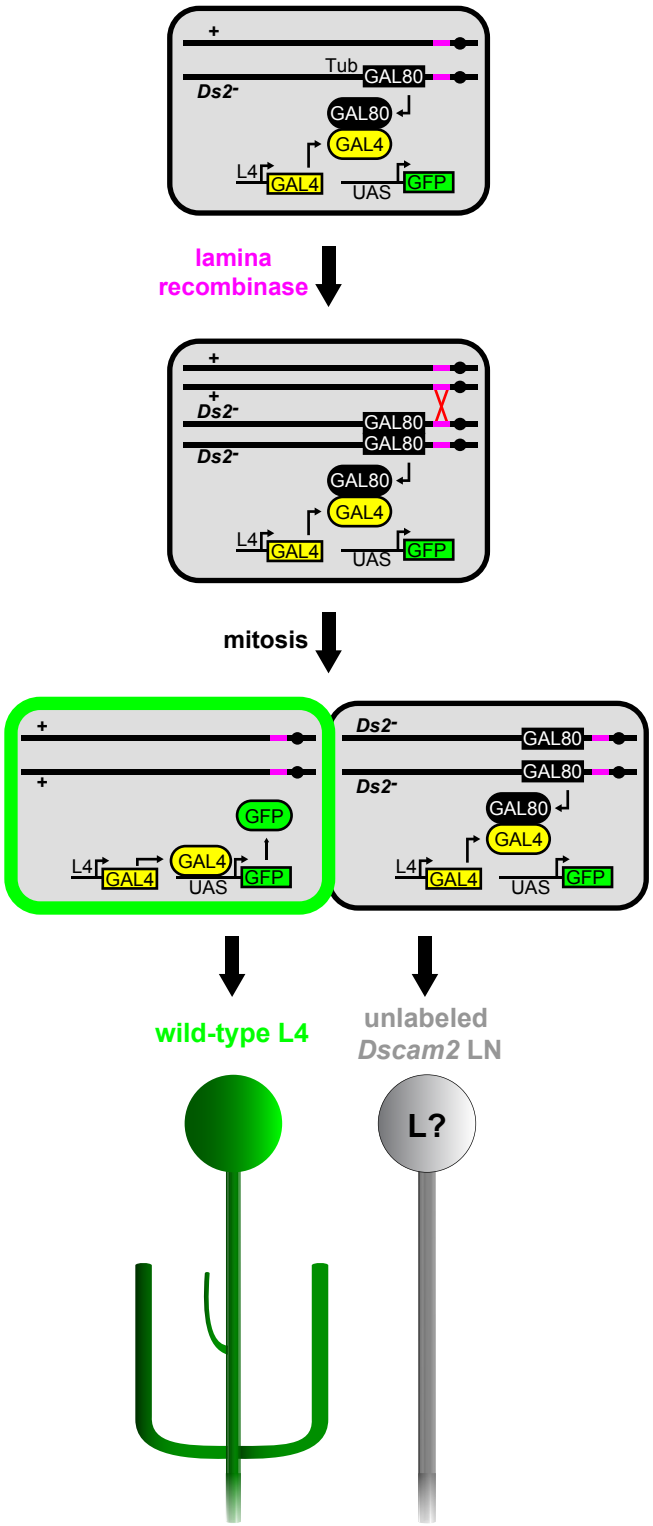

B

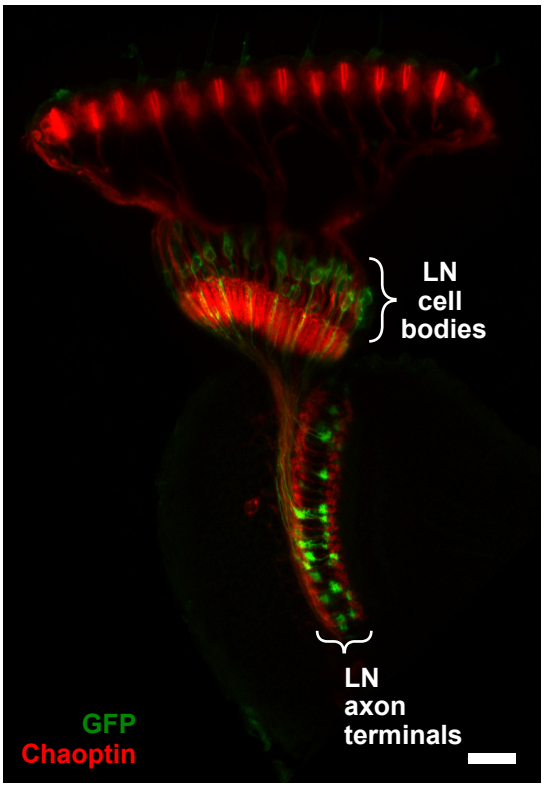

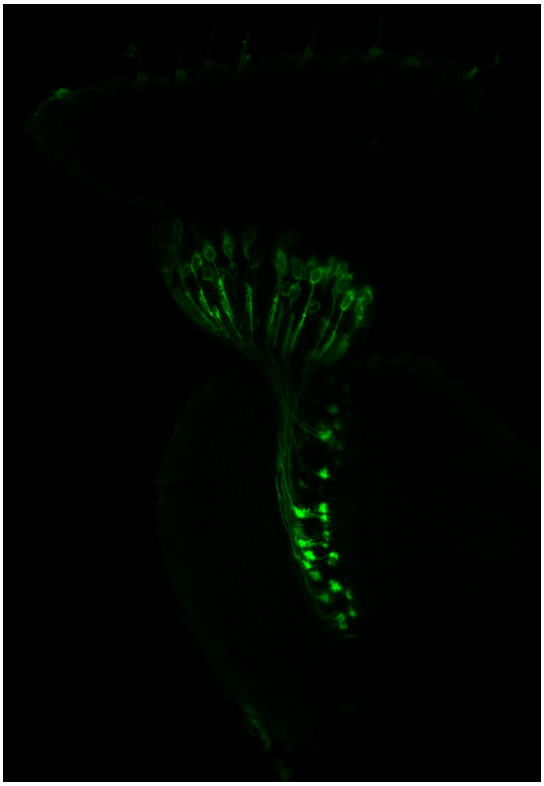

Fig. S4

Dual Label MARCM (DL-MARCM)

L4 - L4 interactions

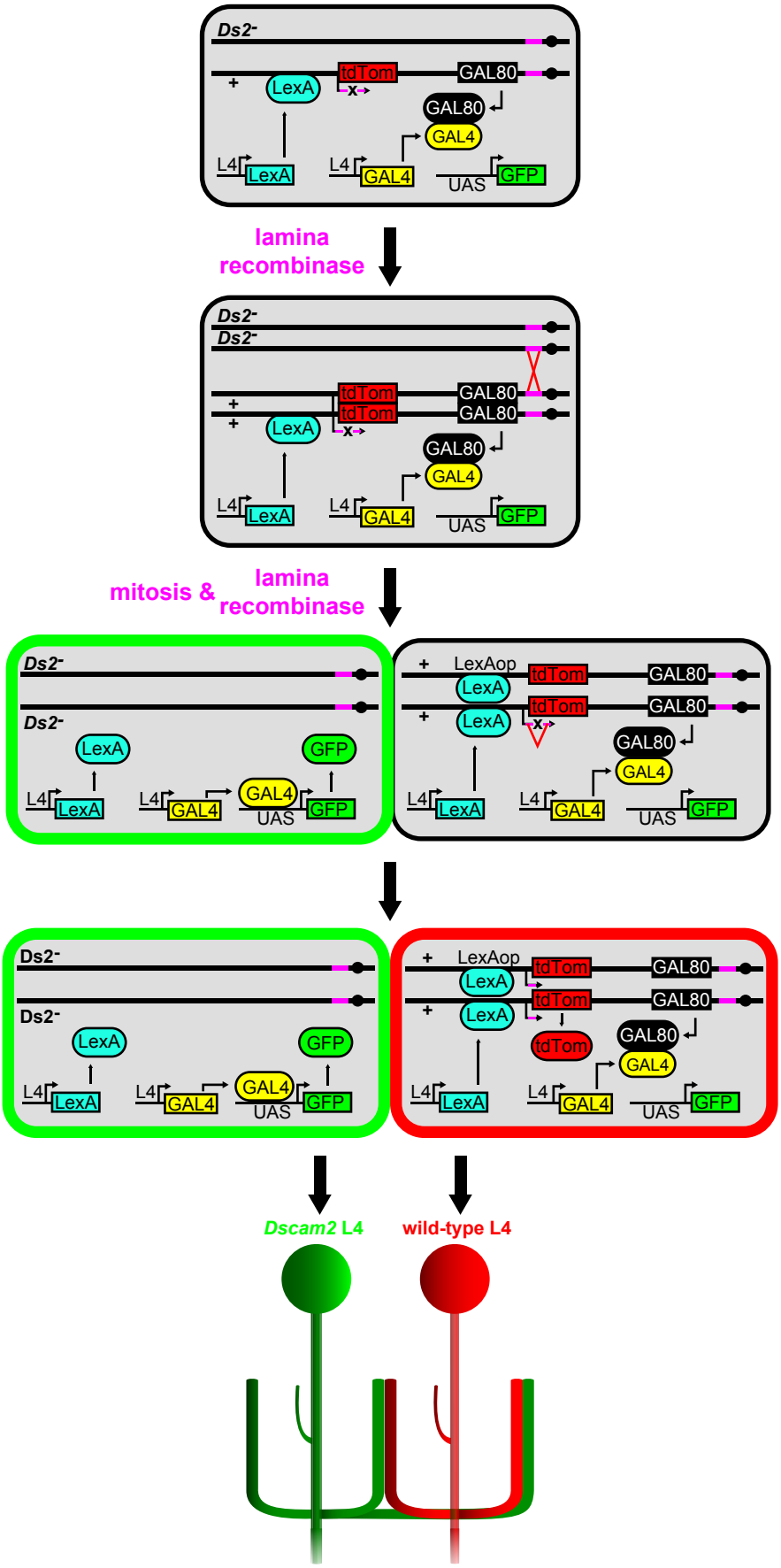

Dscam2 L4 wild-type L4

Fig. S5

DL-MARCM: observed phenotypes

L4 displays +1 phenotype

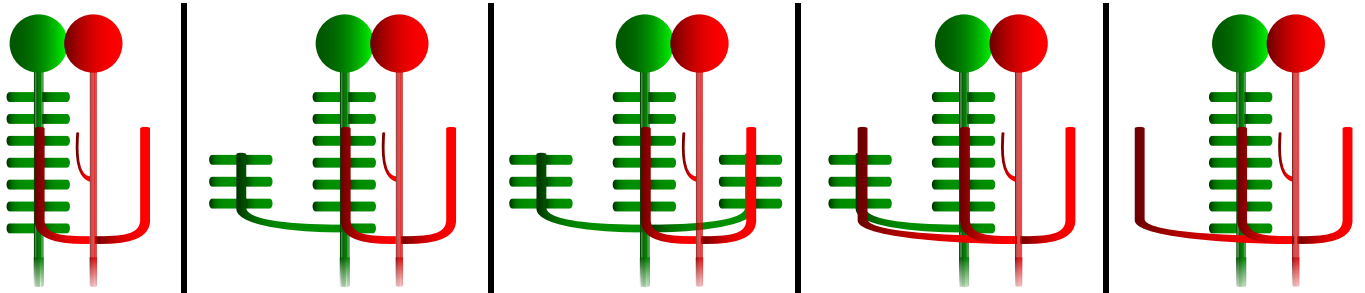

						Total
wild-type MARCM L2	25	0	0	0	0	25
Dscam2 MARCM L2	14	17	1	5	0	37
wild-type MARCM L1	17	0	0	0	0	17
Dscam2 MARCM L1	26	2	0	1	1	30

Fig. S6

Dual Label MARCM (DL-MARCM)

L4 - R Cell interactions

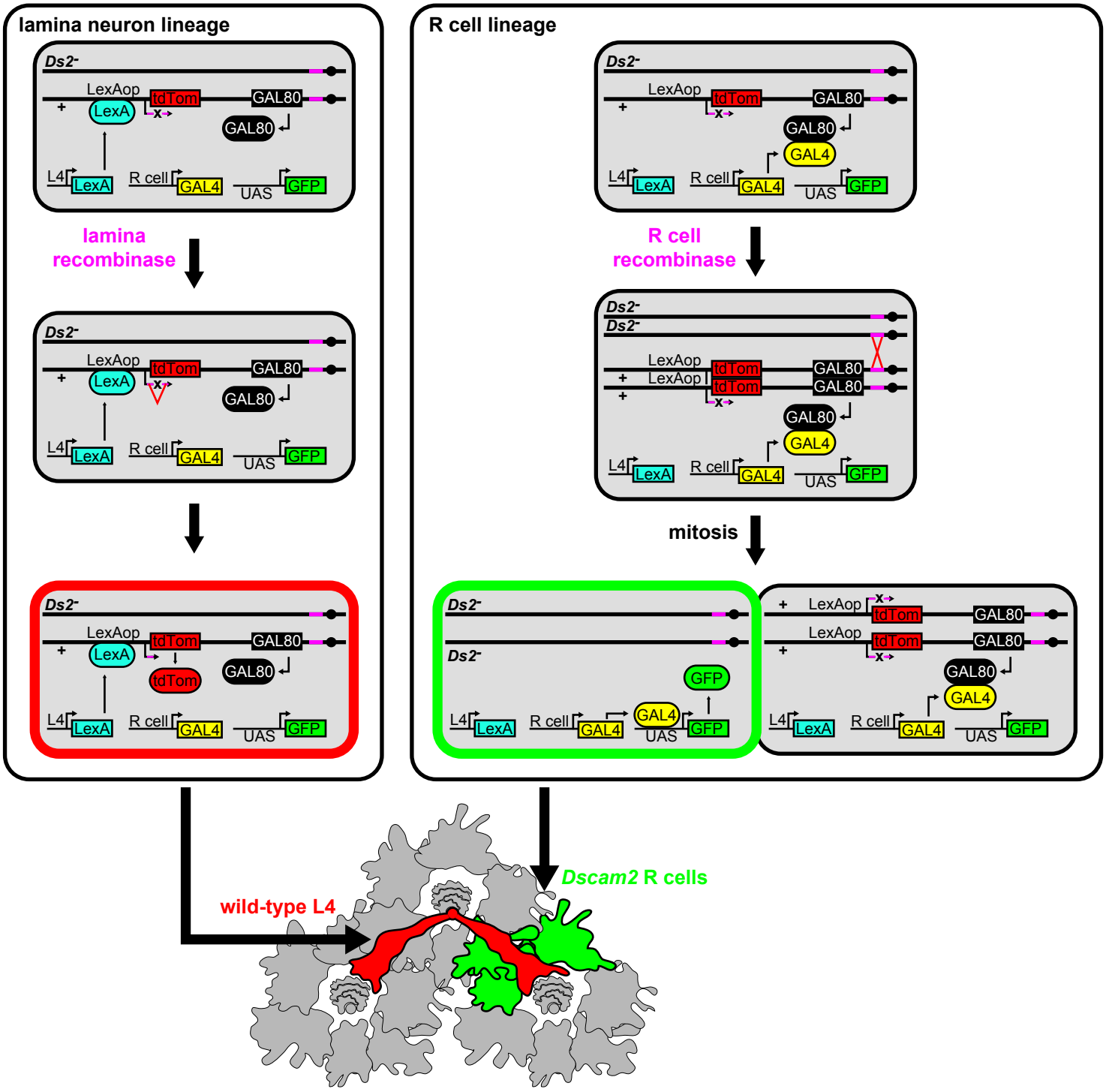

Fig. S7

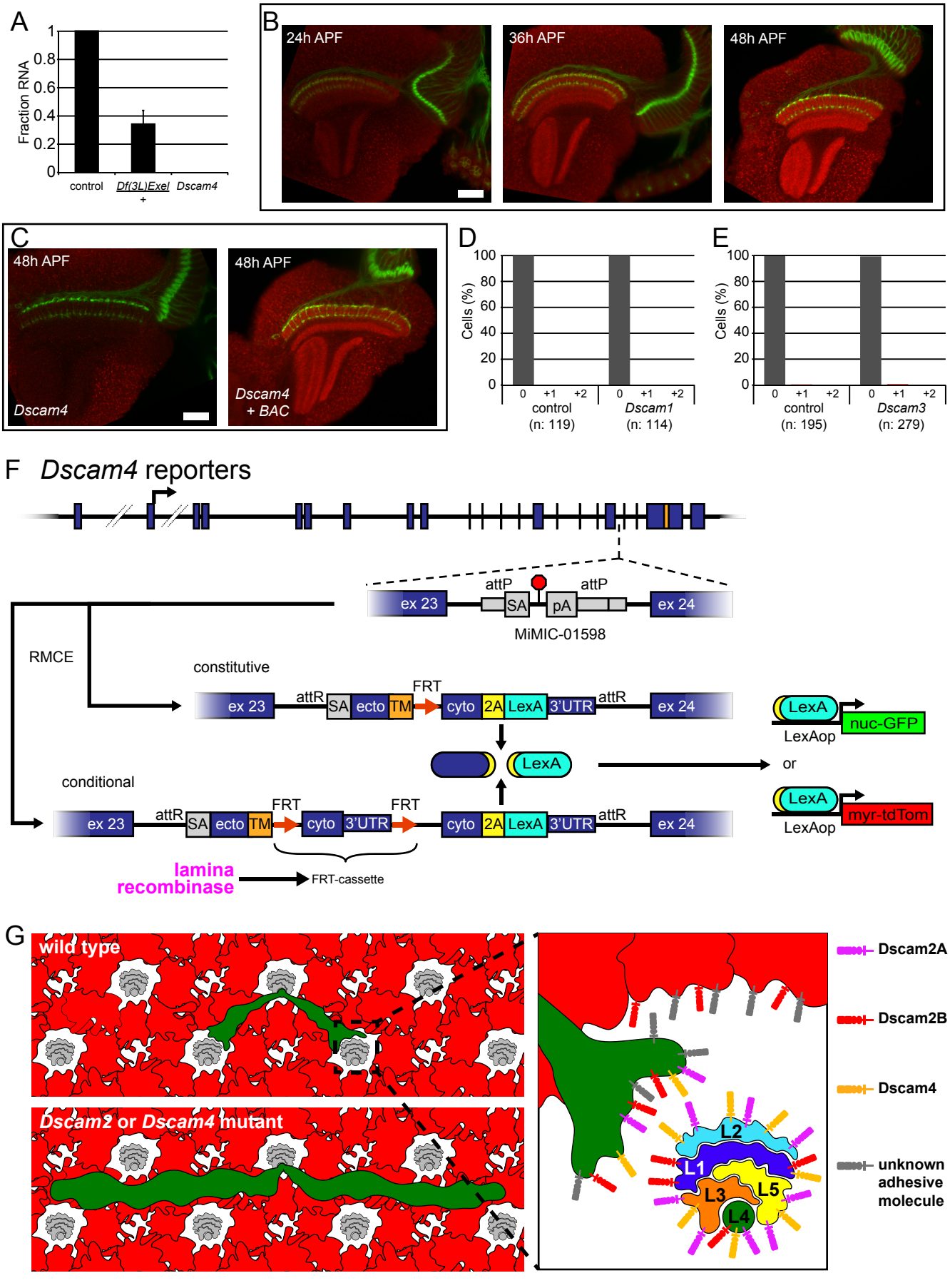
A
Fraction RNA
1
0.8
0.6
0.4
0.2
0
control
Df(3L)Exel +
Dscam4
B
24h APF
36h APF
48h APF
C
48h APF
Dscam4
48h APF
Dscam4 + BAC
D
Cells (%)
100
80
60
40
20
0
0 +1 +2
control
(n: 119)
Dscam1
(n: 114)
E
Cells (%)
control
(n: 195)
Dscam3
(n: 279)
F Dscam4 reporters
ex 23
attP
SA
pA
attP
ex 24
MiMIC-01598
RMCE
constitutive
attR
SA
ecto
TM
FRT
cyto
2A
LexA
3'UTR
attR
LexA
LexAop
nuc-GFP
or
myr-tdTom
conditional
FRT
FRT
lamina recombinase
FRT-cassette
G
wild type
Dscam2 or Dscam4 mutant
Dscam2A
Dscam2B
Dscam4
unknown adhesive molecule
L1
L2
L3
L4
L5

Supplemental Figures

Figure S1. L4 dendritic development after initial targeting step, Related to Figure 2

(A-E) MCFO was used to simultaneously label two adjacent L4 neurons during the developmental stages indicated. Confocal sections (top panels; MIP, maximum intensity projection) were used to generate 3D renderings of L4 neurons (bottom 3 panels in A; bottom panels in B-E). Renderings of R cell growth cones are shown A and B. Dotted lines in C-E indicate proximal and distal boundaries of the R cell terminals. Axons (Ax) are demarcated. Arrowheads in D indicate nascent anterior dendrites. Immunofluorescent signals from the MCFO epitopes were false colored in green and blue. Counterstain (red) is either anti-Chp (A, C, D) or anti-Hiw (E). Anti-Chp staining omitted at 36 h APF MIP for clarity(B). Scale bar, 5 μm.

Figure S2. Dscam2A and Dscam2B are expressed with distinct spatial and temporal specificity and either is sufficient for dendritic targeting at 24 h APF, Related to Figure 3

(A) Schematic of the generation and splicing alternatives of Dscam2A isoform reporter. Homologous recombination was used to replace the *Dscam2* variable region with a mini-*w* selection marker (purple box) flanked by attP landing sites (Lah et al., 2014). These sites where then used to insert sequences that report isoform splicing via recombinase-mediated cassette exchange (RMCE). Shown here is the Dscam2A isoform reporter: Sequences encoding the 2A self-cleaving peptide (yellow box) and the LexA transcriptional activator (cyan box) were fused in frame with exon 11. Addition of a single base pair in exon 10B causes a frameshift such that whenever 10B is spliced it leads to an out-of-frame stop codon in exon 11 resulting in no translation of LexA. Splicing of 10A, however, results in the production of LexA, which is separated from the N-terminal Dscam2 protein by the 2A peptide. LexA is then free to activate transcription of nuc-GFP. Dscam2B reporter (not shown) differs by having an analogous frameshift mutation in exon 10A.

(B) Dscam2A (left panels) and Dscam2B (right panels) isoform reporters label distinct subsets of lamina neurons with nuclear envelope localized GFP (nuc-GFP; green) at the stages indicated. Bsh immunofluorescence (red) highlights nuclei of L4 and L5 cells. 'R' denotes the retina. The arrangement of lamina neuron cell bodies is schematized below each immunofluorescence image. Scale bar, 15 μm.

(C) Dscam2B driving nuc-GFP (green) in the retina at 24 and 48 h APF. R1-R8 were identified based on their positions relative to R3 and R4. These cells were marked with mδ-GAL4 driving myr-tdTom (red) which is expressed weakly in R3 and strongly in R4. Neuronal nuclei were stained with anti-ELAV (magenta). Scale bar, 5 μm.

(D) Schematic of Dscam2 protein tag (top) where V5 and HA epitopes were inserted in frame with exons 10A and 10B resulting in internally tagged protein isoforms. Immunofluorescence against these epitopes at 24 h APF (bottom left) reveals the same cell-type specific Dscam2 isoform expression as reporters in Figure S2B. The arrangement of lamina neuron cell bodies is schematized (bottom right). Note that as this strategy tags Dscam2 protein the lamina neuron dendrites, which are positioned immediately proximal to L5 cell bodies, are also labeled. Scale bar, 15 μm.
(E) MARCM analysis of L4 neurons with *Dscam2* isoform-specific alleles shows that either isoform is sufficient to promote dendritic targeting at this stage.
(F) Dscam2A isoform reporter driving nuc-GFP (green) in the background a wild-type (left panel) and *Dscam2Bstop* allele (right panel) at 24 h APF. No premature expression of Dscam2A in L4 occurs in the presence of *Dscam2Bstop*. Bsh immunofluorescence is in red. The arrangement of lamina neuron cell bodies is schematized below each image. Scale bar, 15 μm.

Figure S3. Reverse MARCM, Related to Figure 4A
(A) Schematic of the generation of mitotic clones of wild-type L4 neurons in the background of unlabeled *Dscam2* lamina neurons (see Table S1 for detailed genotypes). Here, GAL80 (black box) is placed in *cis* to the *Dscam2* mutation. A highly active lamina recombinase was then used to induce mitotic recombination between homologous chromosomes resulting in a homozygous wild-type cell that has lost GAL80. This frees L4-driven GAL4 (yellow box) to activate GFP (green box) thereby highlighting this L4 neuron. The sibling cell, which is homozygous for *Dscam2*, is unlabeled.
(B) Demonstration of the specificity of lamina recombinase. A specific genomic fragment, 27G05, fused to FLP restricts recombination to lamina neurons. Shown here is the retina and optic lobe from a 48 h APF pupa carrying a GFP reporter for FLP activity (green; top and bottom panels) counterstained with anti-Chp (red; top panel). See Table S1 for detailed genotype. Scale bar, 15 μm.

Figure S4. Dual Label MARCM (DL-MARCM) for L4 – L4 interactions, Related to Figure 4B-D
Schematic showing the dual labeling of a wild-type and *Dscam2* L4 neurons (see Table S1 for detailed genotypes). Here a highly active lamina recombinase induces two forms of labeling. The first is achieved through standard MARCM; upon induction of mitotic recombination between homologous chromosomes, a cell homozygous for *Dscam2* is produced that lacks GAL80 (black box) allowing L4-driven GAL4 (yellow box) to activate GFP (green box) transcription and label this cell in the green channel. The sister cell, on the other hand, still has GAL80 and therefore has no GFP labeling. The second labeling scheme occurs when lamina recombinase also removes the interruption cassette ('x') upstream of myr-tdTom (red box) resulting in the labeling of wild-type and heterozygous L4 cells in the red channel. Since the myr-

tdTom transgene is linked to the wild-type *Dscam2* allele (*i.e.* on the same chromosomal arm), in no case will a homozygous mutant cell be labeled with myr-tdTom. For testing interactions between L4 neurons and those in the target fascicle (see Figure 4C, D), an L1-L2-GAL4 was used in place of L4-GAL4.

Figure S5. DL-MARCM: observed phenotypes, Related to Figure 4C, D
Phenotypes of MARCM (green) and FLP-out (red) lamina neurons observed in DL-MARCM experiments with L2 and L1. Removal of *Dscam2* from L2 or L1 will result in an ectopic branch phenotype in these cells as previously reported (Lah et al., 2014).

Figure S6. DL-MARCM for L4 – R cell interactions, Related to Figure 5
Schematic of the generation of labeled wild-type L4 neurons in the background of *Dscam2* MARCM clones of R cells (see Table S1 for detailed genotypes). This scheme relies on lamina and R cell recombinases, expressed and active in the two separate lineages that derive each cell class. Wild-type L4 neurons are labeled by an L4-driven LexA (cyan box) which activates transcription of myr-tdTom (red box). This activation is normally blocked by an FRT (purple bar)-flanked interruption cassette ('x'). The weakly active lamina recombinase excises this interruption cassette in a stochastic manner allowing for L4 cells to be labeled with myr-tdTom. Standard MARCM (R cell lineage) is used to generate R cells mutant for *Dscam2*; *Dscam2* mutation is placed in *trans* to the GAL80 repressor (black box) such that in heterozygous cells GAL80 blocks the activity of R cell-driven GAL4 (yellow box). The highly active R cell recombinase induces mitotic recombination between FRT sites on homologous chromosomes allowing for the production of homozygous *Dscam2* cells, which have lost GAL80. This frees GAL4 to drive expression of GFP (green box) thereby marking these mutant R cells.

Figure S7. *Dscam4* allele characterization and model for L4 dendritic targeting, Related to Figure 6
(A) qPCR analysis of Dscam4 RNA levels in adults. Animals heterozygous for *Df(3L)Exel6112,* which is a chromosomal deficiency that removes *Dscam4*, were used as a positive control of our assay. Fraction of RNA in extracts relative to wild-type controls shown in graph.
(B, C) Immunofluorescence of Dscam4 (red) in optic lobes at the indicated stages and genotypes. (B) Dscam4 expression in optic lobe neuropils increases from 24-48 h APF. (C) Dscam4 immunostaining signal is lost in *Dscam4* homozygous animals (left panel) and restored in the presence of a bacterial artificial chromosome (BAC) containing the *Dscam4* gene (right panel). Anti-Chp staining of R cell axons is in green. Scale bar, 25 μm.

(D, E) MARCM analysis of adult L4 neurons using alleles for *Dscam1* (D) and *Dscam3* (E). In the absence of a null mutation specific for *Dscam3*, a small chromosomal deficiency (*Df(3R)BSC743*) that removes this paralog along with 8 other genes was used.
(F) Schematic of the generation and manipulation of Dscam4 reporters. RCME was used to insert sequence encoding two versions of the reporter using the attP sites in the Mi01598 insertion. The constitutive version consists of a splice acceptor (yellow box) fused to the remainder of the Dscam4 coding sequence followed by 2A-LexA (as in the Dscam2 reporters). The conditional version differs only by having a cassette sequence flanked by FRT recombination sites. In the absence of FLP recombinase activity, translation of Dscam4 ends with no reporter produced. When a lamina specific recombinase is present, this FRT-cassette is excised and 2A-LexA is produced only in lamina neurons. Either nuc-GFP or myr-tdTom were used as readouts of LexA activity.
(G) Model for L4 dendritic targeting. In the wild type (top panel), L4 dendrites use Dscam2 and Dscam4 to adhere to multiple lamina neurons in the target fascicle. Abrogation of Dscam2 or Dscam4 function (bottom panel) results in dendritic mistargeting. We propose that in the absence of Dscam2 or Dscam4, a weaker adhesive interaction between L4 dendrites and R cell growth cones is uncovered (symbolized in the figure by grey molecule). This leads to a tight association between them.
Isoform reporters revealed that each lamina neuron exclusively expresses a single Dscam2 isoform as indicated (right panel). Although Dscam2A was not detected in L4 dendrites at 24 h APF, sufficient Dscam2A must be produced in these neurons to promote normal targeting as L4 neurons lacking Dscam2B target normally (see text). That is, either Dscam2A or Dscam2B is sufficient in L4 to promote normal targeting. This is consistent with a redundant function of L1 and L2 neurons in directing L4 targeting by homophilic binding, as each expresses a different isoform. It remains unclear, however, why removal of Dscam2 from L1 or L2 leads to L4 targeting defects, albeit with incomplete penetrance, while L4 dendrites lacking Dscam2A or Dscam2B target normally. This discrepancy may reflect additional factors contributing to interactions between L4 dendrites and the target fascicle, including the position of different lamina axons within the target fascicle and the relative expression levels of the isoforms on the surface of these neurons.

Supplemental Movies

Movie S1. Live imaging of wild-type L4 neurons, Related to Figure 7A

Dendritic targeting occurs in three phases: exploratory, anchoring and consolidation (see Figure 7A). MARCM-generated wild-type L4 neurons (cyan) imaged live from 16-26 h APF. R cell marker (red) in the left panel is inverted in the right panel to reveal positions of the lamina fascicles. Each frame is a MIP

in the region of the lamina plexus taken every 13 min (see Supplemental Experimental Procedures). In both channels, each frame was individually contrast enhanced. L4 neurons are displayed with a cyan-hot look-up table to capture more of the dynamic range with limited saturation. The R cell channel was processed to reduce local variations in signal intensity.

Movie S2. Live imaging of *Dscam2* mutant L4 neurons, Related to Figure 7B

In *Dscam2* mutants, after an exploratory phase similar to wild type, dendritic anchoring does not occur. Instead dendrites extend significant distances along the D-V axis. MARCM-generated *Dscam2* mutant L4 neurons and R cells displayed as in Movie S1.

Table S1. Complete genotypes used in each figure, Related to Experimental Procedures

Mutations and transgenes present on each chromosome used every data figure.

Fig.	X chromosome	2nd chromosome	3rd chromosome
1G, 6E	27G05[1]-FLP1(attP18) y/+	*ap*[2]-GAL4 UAS-CD8-GFP +	*tub*-GAL80 Frt79 [x] Frt79
1H	27G05-FLP2(attP18) y/+	*ap*-GAL4 UAS-CD8-GFP +	*tub*-GAL80 Frt79 [x] Frt79
2B, S1	27G05-FLP2(attP18) y/+	*ap*-GAL4 +	pJFRC201 pJFRC240[3] +
2C	27G05-FLP2(attP18) y/+	*ap*-GAL4 +	pJFRC201 pJFRC240* *svp*-GAL4
3B, 6F, S2E	27G05-FLP2(attP18) y/+	*ap*-GAL4 10xUAS-myr-GFP	*tub*-GAL80 Frt79 [x] Frt79
S2B	+ y/+	+ +	Dscam2[A/B]-LexA LexAop-nuc-GFP +
S2C	+ y/+	+ +	Dscam2[A/B]-LexA LexAop-nuc-GFP mδ[4]-GAL4 UAS-myr-TdTom
4A	27G05-FLP2(attP18) y/+	*ap*-GAL4 UAS-CD8-GFP +	Frt79 [x] *tub*-GAL80 Frt79
4B	Dac[5]-FLP y/+	Dac-FLP20 *ap*-GAL4 UAS-CD8-GFP	[x] Frt79 L4-LexA LexAop-FSF-myr-tdTom *tub*-GAL80 Frt79
4C,D	Dac-FLP y/+	Dac-FLP20 L1-L2-GAL4 UAS-CD8-GFP	[x] Frt79 L4-LexA LexAop-FSF-myr-tdTom *tub*-GAL80 Frt79
5C,D	ey3.5FLPG5D[6] y/+	Dac-FLP20 GMR-GAL4[7] 10xUAS-myr-GFP	[x] 9B08[8]-GAL4 Frt79 L4-LexA LexAop-FSF-myr-tdTom *tub*-GAL80 Frt79
6B	27G05-FLP2(attP18) y/+	*ap*-GAL4 UAS-CD8-GFP +/BAC	*tub*-GAL80 Frt79 [x] Frt79
6C (left)	+ y/+	+ +	Dscam4-LexA-constitutive LexAop-myr-tdTom
6C (right)	+ y/+	Dac-FLP20 +	Dscam4-LexA-conditional LexAop-FSF-myr-tdTom
6D	+ y/+	+ +	Dscam4-LexA-constitutive LexAop-nuc-GFP mδ-GAL4 UAS-myr-tdTom
7A,B, Mov S1,S2	27G05-FLP2(attP18) y/+	*ap*-GAL4 10xUAS-myr-GFP GMR-myr-tdTom	*tub*-GAL80 Frt79 [x] 10xUAS-myr-GFP (attP2) Frt79
S2F	+ y/+	+ +	Dscam2A-LexA LexAop-nuc-GFP +/*Dscam2Bstop*
S3B	27G05-FLP2(attP18) y/+	A5C-FSF-GAL4 10xUAS-myr-GFP +	+ +
S7C	+ y/+	+ +/BAC	*Dscam4*^{Mi01598} *Dscam4*^{Mi01598}
S7D	27G05-FLP1(attP8) y/+	Frt42D *tub*-GAL80 A5C-GAL80 Frt42D [x]	L4-GAL4 UAS-myr-tdTom +
S7E	27G05-FLP1(attP8) y/+	*ap*-GAL4 UAS-CD8-GFP +	Frt82B *tub*-GAL80 Frt82B [x]

[x] denotes control or mutations as specified in figures

[1]in the visual system 27G05 is active only in lamina neuron precursors (see Figure S3B)

[2]*ap* is active in L4

[3]see Supplemental Experimental Procedures for full genotype

[4]mδ is highly active in R4 and weakly in R3

[5]Dac is active in lamina neuron precursors

[6]ey3.5FLPG5D is active R cell precursors and occasionally in the lamina (see Supplemental Experimental Procedures)

[7]GMR-GAL4 is active in R cells

[8]9B08 is active in all lamina neurons

Supplemental Experimental Procedures

Fly Stocks

Complete genotypes used in each experiment are detailed in Table S1. Flies were reared and staged at 25°C using standard protocols.

The following fly lines were used: *Dscam2*$^{null-1}$, Dac-FLP (X), Dac-FLP20 (Millard et al., 2007); *Dscam1*^{23} (Hummel et al., 2003); *Dscam4*^{Mi01598} (Venken et al., 2011); *ap*-GAL4(md544), *tub*-GAL80 (2R, 3L, 3R), UAS-CD8-GFP, *Df(3L)Exel6112*, *Df(3R)BSC743*, 10xUAS-myr-GFP (attP2; attP40), 10xUAS-myr-tdTom (attP2), GMR-GAL4, A5C-FSF-GAL4 (Bloomington Stock Center); L1-L2-GAL4 (Rister et al., 2007); *svp*-GAL4 (*Drosophila* Genetic Resource Center); 27G05-FLP1 (attP8, attP18), 27G05-FLP2 (attP18), L4(31C06)-GAL4, L4(31C06)-LexA, 9B08-GAL4 (gifts from Gerald Rubin); A5C-GAL80 (gift from Barret Pfeiffer and Gerald Rubin; Pfeiffer et al., 2010); pJFRC201 pJFRC240 (see below for details; gift from Aljoscha Nern); LexAop-nuc-GFP (gift from Gilbert Henry; Henry et al., 2012); mδ-GAL4 (gift from Tom Clandinin; Chen and Clandinin, 2008); ey3.5FLPG5D (Pecot et al., 2014); LexAop-myr-tdTom (attP2; Chen et al., 2014); LexAop-FSF-myr-tdTom, GMR-myr-tdTom (see below for information on their construction).

Mosaic Analysis

Single cell mosaic analyses were done with genotypes listed in Table S1. Mitotic clones in lamina neurons were generated using either of two different genomic fragments, 27G05 (Pecot et al., 2013) or Dac (Millard et al., 2007), driving FLP1 or FLP2 recombinase. L4 neurons were labeled with either *ap*-GAL4 or L4(31C06)-GAL4. R cell mitotic clones were generated with ey3.5FLPG5D and labeled with GMR-GAL4. Since ey3.5FLPG5D occasionally generates mitotic clones in lamina neurons, we made sure that these were not present near the areas of the brain examined in our DL-MARCM experiment by including 9B08-GAL4, a reporter active in all lamina neurons (Pfeiffer et al., 2008). Sporadic FLP-out L4 clones were generated with Dac-FLP and LexAop-FSF-myr-tdTom.

LexAop-FSF-myr-tdTom: An 823 bp fragment containing SV40 polyA flanked by FRT was PCR amplified and inserted downstream of the LexAop promoter in LexAop-myr-tdTom (Chen et al., 2014). This was inserted into attP2 using site-directed transformation (Bestgene).

Generation of Dscam2 isoform-specific alleles

DNA Constructs

We used a previously described a plasmid carrying wild-type *Dscam2* sequence spanning exons 9-11 flanked by attB sites (pCR4 attB Control; Lah et al., 2014) as a template for producing PCR products that

contain stop codons in the variable exon 10 alternates. We also took advantage of the fact that this plasmid has only two AccI sites, with one positioned upstream of the intended stop codon site in exon 10A (AccI#1) and one positioned immediately downstream of that in exon 10B (AccI#2).

Dscam2Astop: Two fragments which overlap within a 16 bp region of exon 10A TCGCTCACCTGTTCGG were PCR amplified from pCR4 attB Control. The 5' fragment initiated just upstream of AccI#1 while the 3' fragment extended just downstream of AccI#2. The primers used to generate the overlapping region within exon 10A carried a single base substitution (C→A) such that resulting overlap region was TAGCTCACCTGTTCGG, which would convert Ser-631 to a stop codon. These two fragments were fused together using overlap extension (OE-)PCR and the resulting product was subcloned into pCR4 attB Control with AccI to yield a plasmid carrying a single stop codon in exon 10A. We confirmed that this this fragment inserted with correct orientation by PCR.

Dscam2Bstop: The same approach was used to generate Dscam2Bstop with the exception that the overlap region was a 16 bp region within exon 10B: GCATTCCGTCGCTGTC. OE-PCR using primers with two substituted bases converted this region to GCATTCCGTAGCTGTA resulting in two nonsense mutations (underlined) in place of Ser-675 and Ser-677.

Dscam2A+Bstop: Likewise, OE-PCR was used to fuse three fragments with the above overlaps in exon 10A and 10B using the same modified primers. This resulted in a final construct containing the above three nonsense mutations in both alternative exons.

Transformation

These three constructs were used to transform the *Dscam2* founder line (Genetivision; Lah et al., 2014). This fly line contains a mini-*w*+ gene flanked by attP sites in place of endogenous exons 9-11 in *Dscam2* (Figure S2A). RMCE was used to swap in sequences with engineered nonsense mutations. Transformants were identified based on the loss of the *w*+ marker. Genomic DNA from the transformants was used to confirm the correct orientation and sequence of the inserted fragments.

Multicolor Flip Out (MCFO) labeling

MCFO (Nern et al., 2015) was performed using *ap*-GAL4 (and *svp*-GAL4 for additional L1 labeling) and 27G05-FLP2 stochastically acting on 3 different UAS-reporters contained within the following transgenes:

pJFRC201: 10XUAS-FSF-myr-smGFP-HA (VK00005)

pJFRC240: 10XUAS-FSF-myr-smGFP-V5-THS-10XUAS-FSF-myr-smGFP-FLAG (attP1)

Each reporter consists of a non-fluorescent GFP backbone (smGFP; sm, spaghetti monster) acting as a scaffold for multiple copies of V5, HA or FLAG. Each epitope was detected using a different fluorescent

secondary antibody. Stochastic recombination resulted in L4 (and L1) neurons expressing seven different fluorescent signatures.

Live Imaging and Image Processing

Robust labeling of early (<24 h APF) L4 neurons was achieved by using a UAS-myr-GFP transgene *in trans* to GAL80 such that this transgene becomes homozygous in MARCM-generated L4s. We suspect that the resulting strong expression of GFP, estimated to be >20 fold higher than other placements of this transgene, is due to transvection between the two homologous chromosomes (Mellert and Truman, 2012).

Data were acquired with a custom-built microscope equipped with 2 GaAsP detectors (Hamamatsu) and a long working distance water immersion objective (Zeiss, W Plan-Apochromat 20x/1.0 DIC). A tunable Ti:sapphire pulsed laser (Chameleon Ultra II, Coherent) was used for excitation (970 nm for tdTom+GFP imaging, ~25 mW). Pupae were attached eye-down on the cover glass after removal of the cuticle around the head. Animals were staged at head eversion (12 h APF) and kept at 25°C using an objective heater system (Bioptechs).

Two-channel volume stacks of the lamina acquired every 13 minutes over ~10 hours of development were processed to stabilize the tissue against developmental and mechanical drift. Maximum intensity projections restricted to the lamina plexus were generated using computed surface fits to the neuropil as masks. Image processing and analysis was carried out with custom software written in Matlab (Mathworks). Several critical scripts were sourced from the Mathworks File Exchange repository (D'Errico, 2005, 2009; Kroon, 2008). Fiji (Schindelin et al., 2012) was used for batch processing and user-assisted tasks. Detailed information on image processing is available upon request.

GMR-myr-tdTom construct: The vector, pGMRTattB, was generated by replacing the UAS sequences in pUASTattB with the GMR promoter element (Hay et al., 1994) using restriction cloning. To prepare the insert, myristoylation sequence of Src64B (nt 1-255) was amplified from genomic DNA and joined to the 5' end of the tdTom ORF with restriction cloning. The fused product was subcloned into the vector MCS between the EcoRI and NotI sites. The construct was incorporated into the fly genome at the attP5 landing site with phiC31-mediated recombination (Bestgene).

Generation of Transgenic Expression Lines

DNA Constructs

Dscam2A-LexA and Dscam2B-LexA: These isoform reporters are essentially identical to those by Lah *et al.* (2014) with the exception that LexAp65 is used instead of GAL4. First, OE-PCR was used to generate a fragment joining 2A, LexAp65 and SV40 polyA sequences flanked by NheI and AgeI sites. These restriction enzymes were then used to subclone this fragment into the corresponding sites in pCR4 attB

10A^{fs}-2AGAL4 and pCR4 attB 10B^{fs}-2AGAL4 (Lah et al., 2014) to generate pCR4 attB 10A^{fs}-2ALexA and pCR4 attB 10B^{fs}-2ALexA, respectively.

Dscam4 constitutive reporter: OE-PCR was used to fuse sequences encoding a splice acceptor, Dscam4 cDNA encompassing exon 24 - TM domain (labeled as SA, ecto and TM, respectively in Figure S7F) and a glycine-serine linker (GS). This fragment was subcloned into XbaI and EcoRI sites present on our previously modified pBS-KS-attB1-2-GT-SA plasmid (Pecot et al., 2013). To this resultant plasmid, a PCR fragment containing the Dscam4 3'UTR followed by 129 bp of downstream genomic DNA was subcloned between the HindIII and NotI sites. Next a fragment containing FRT-3xV5-GS was inserted between the EcoRI and HindIII sites (not shown in Figure S7F). This V5 epitope was used to verify the neuropil localization of tagged Dscam4 protein but was otherwise not used no determining cellular expression. Finally, OE-PCR was used to produce fragment fusing the Dscam4 cytodomain to 2A-LexAp65, which was then subcloned into the XhoI and HindIII sites.

Dscam4 conditional reporter: OE-PCR was used to produce a fragment fusing FRT, GS, Dscam4 cytodomain and 3'UTR. This was then subcloned into the EcoRI site in the Dscam4 constitutive reporter producing an FRT-flanked cassette that can be removed in the presence of FLP recombinase.

Transformation

The pCR4 attB 10A^{fs}-2ALexA,pCR4 attB 10B^{fs}-2ALexA and pCR4 attB A-V5 B-HA constructs were used to transform the *Dscam2* founder line using RCME (as above) to produce the Dscam2B and Dscam2A isoform reporters, respectively. The Dscam4 expression constructs were used to transform *Dscam4^{Mi01598}* flies by RCME (Bestgene). Transformants were identified based on loss of yellow+ marker. Correctly orientated insertions were verified by PCR and sequencing from genomic DNA of transformed flies.

Immunostaining

Immunostaining was performed as described previously (Nern et al., 2008) with minor modification. Fly brains were fixed at room temperature with PLP (4% paraformaldehyde, 75 mM lysine, 37 mM sodium phosphate buffer pH 7.4) for 20 min (24 h APF brains) or 25 min (brains older than 24 h APF). Samples were incubated with primary and secondary antibodies for 2 days each at 4°C. Brains were mounted in EverBrite medium (Biotium).

The following primary antibodies were used in this study: chicken anti-GFP (1:500, RRID:AB_300798) and chicken anti-V5 (1:400, RRID:AB_307022) were from abcam; guinea pig anti-Dscam4 (1:5000; this study – see below), guinea pig anti-Bsh (1:500; Hasegawa et al., 2011), rabbit anti-DsRed (1:200; Clontech, RRID:AB_10015246); rabbit anti-HA (1:300; Cell Signaling Technologies, RRID:AB_1549585); rat anti-FLAG (1:200; Novus Biologicals, RRID:AB_1625981); mouse anti-Hiw

(1:20, RRID:AB_528277), mouse anti-Chp (1:20, RRID:AB_528161), rat anti-ELAV (1:500, RRID:AB_528218) were from Developmental Studies Hybridoma Bank (DSHB). The following secondary antibodies were used: anti-chicken Alexa 488 (RRID:AB_142924), goat anti-rat Alexa 647 (1:150, RRID:AB_10563568), anti-mouse Alexa 488 (RRID:AB_138404), anti-chicken Dylight 550, anti-mouse Alexa 647 (RRID:AB_141725, Life Technologies); anti-mouse Cy3 (RRID:AB_2338699), donkey anti-guinea pig Cy3 (RRID:AB_2340460), anti-rabbit Cy3 (RRID:AB_2338011), donkey anti-rabbit Alexa 594 (RRID:AB_2340621, Jackson ImmunoResearch Laboratories). If not otherwise specified, all secondary antibodies were used at 1:500 and raised in goat.

Quantitative PCR (qPCR)

RNA was extracted from adult male flies using an RNeasy mini kit (Qiagen). cDNA was produced using SuperScript III First-Strand Synthesis System (Invitrogen). Primers against Dscam4 cDNA (GCTCCACTTCGATCTATATCACC, GGATCGGTTTCGTACAGCTC) were used with SYBR Green Master Mix in a qPCR reaction on an IQ5 Thermocycler (Bio-Rad). RpL11 transcripts were used as a control for total RNA levels and measured using the following primers: ACATACCACAATGGCGGCGGTTAC, ACGCAGATGTTCAGGCAGAGTTTG. REST 2009 software (Qiagen) was used for analysis of qPCR output.

Dscam4 antibody generation

The entire Dscam4 cytoplasmic domain was gene synthesized using codons optimized for *E. coli* (Genewiz) and cloned into the pT7 MAT-Tag FLAG-1 Expression Vector (Sigma). The resulting plasmid was transformed into BL21 cells and protein was isolated using a nickel column. This protein was then used an antigen in a guinea pig immunization protocol using standard procedures (Thermo Scientific).

Dscam4 BAC generation

The original BAC, CH321-47B15 (BACPAC Resources Center), contained ~84 kb of genomic DNA (3L: 8,198,803-8,282,774; r6.06) encompassing the entire *Dscam4* locus along with ~40 kb of upstream sequence. Most of this upstream sequence was removed using *rpsl*/*kan*-based BAC recombineering (Wang et al., 2009) such that only ~7 kb remained upstream of *Dscam4* (3L: 8,231,709-8,282,774) making this more feasible for subsequent transformation. This shortened BAC was inserted in attP14 using standard site-directed transformation techniques (Bestgene). Transformants were identified based on the appearance of the *white*+ marker.

Supplemental References

Chen, P.-L., and Clandinin, T.R. (2008). The cadherin Flamingo mediates level-dependent interactions that guide photoreceptor target choice in Drosophila. Neuron *58*, 26–33.

Chen, Y., Akin, O., Nern, A., Tsui, C.Y.K., Pecot, M.Y., and Zipursky, S.L. (2014). Cell-type-Specific Labeling of Synapses In Vivo through Synaptic Tagging with Recombination. Neuron *81*, 280–293.

D'Errico, J. (2005). Surface Fitting using gridfit - File Exchange - MATLAB Central.

D'Errico, J. (2009). SLM - Shape Language Modeling - File Exchange - MATLAB Central.

Hasegawa, E., Kitada, Y., Kaido, M., Takayama, R., Awasaki, T., Tabata, T., and Sato, M. (2011). Concentric zones, cell migration and neuronal circuits in the Drosophila visual center. Development *138*, 983–993.

Hay, B.A., Wolff, T., and Rubin, G.M. (1994). Expression of baculovirus P35 prevents cell death in Drosophila. Development *120*, 2121–2129.

Henry, G.L., Davis, F.P., Picard, S., and Eddy, S.R. (2012). Cell type-specific genomics of Drosophila neurons. Nucleic Acids Res. *40*, 9691–9704.

Hummel, T., Vasconcelos, M.L., Clemens, J.C., Fishilevich, Y., Vosshall, L.B., and Zipursky, S.L. (2003). Axonal targeting of olfactory receptor neurons in Drosophila is controlled by Dscam. Neuron *37*, 221–231.

Kroon, D.-J. (2008). B-spline Grid, Image and Point based Registration - File Exchange - MATLAB Central.

Lah, G.J., Li, J.S.S., and Millard, S.S. (2014). Cell-Specific Alternative Splicing of Drosophila Dscam2 Is Crucial for Proper Neuronal Wiring. Neuron *83*, 1376–1388.

Mellert, D.J., and Truman, J.W. (2012). Transvection Is Common Throughout the Drosophila Genome. Genetics *191*, 1129–1141.

Millard, S.S., Flanagan, J.J., Pappu, K.S., Wu, W., and Zipursky, S.L. (2007). Dscam2 mediates axonal tiling in the Drosophila visual system. Nature *447*, 720–724.

Nern, A., Zhu, Y., and Zipursky, S.L. (2008). Local N-Cadherin Interactions Mediate Distinct Steps in the Targeting of Lamina Neurons. Neuron *58*, 34–41.

Nern, A., Pfeiffer, B.D., and Rubin, G.M. (2015). Optimized tools for multicolor stochastic labeling reveal diverse stereotyped cell arrangements in the fly visual system. Proc. Natl. Acad. Sci. *112*, E2967–E2976.

Pecot, M.Y., Tadros, W., Nern, A., Bader, M., Chen, Y., and Zipursky, S.L. (2013). Multiple Interactions Control Synaptic Layer Specificity in the Drosophila Visual System. Neuron *77*, 299–310.

Pecot, M.Y., Chen, Y., Akin, O., Chen, Z., Tsui, C.Y.K., and Zipursky, S.L. (2014). Sequential Axon-Derived Signals Couple Target Survival and Layer Specificity in the Drosophila Visual System. Neuron *82*, 320–333.

Pfeiffer, B.D., Jenett, A., Hammonds, A.S., Ngo, T.-T.B., Misra, S., Murphy, C., Scully, A., Carlson, J.W., Wan, K.H., Laverty, T.R., et al. (2008). Tools for neuroanatomy and neurogenetics in Drosophila. Proc. Natl. Acad. Sci. *105*, 9715–9720.

Pfeiffer, B.D., Ngo, T.-T.B., Hibbard, K.L., Murphy, C., Jenett, A., Truman, J.W., and Rubin, G.M. (2010). Refinement of Tools for Targeted Gene Expression in Drosophila. Genetics *186*, 735–755.

Rister, J., Pauls, D., Schnell, B., Ting, C.-Y., Lee, C.-H., Sinakevitch, I., Morante, J., Strausfeld, N.J., Ito, K., and Heisenberg, M. (2007). Dissection of the Peripheral Motion Channel in the Visual System of Drosophila melanogaster. Neuron *56*, 155–170.

Schindelin, J., Arganda-Carreras, I., Frise, E., Kaynig, V., Longair, M., Pietzsch, T., Preibisch, S., Rueden, C., Saalfeld, S., Schmid, B., et al. (2012). Fiji: an open-source platform for biological-image analysis. Nat. Methods *9*, 676–682.

Venken, K.J.T., Schulze, K.L., Haelterman, N.A., Pan, H., He, Y., Evans-Holm, M., Carlson, J.W., Levis, R.W., Spradling, A.C., Hoskins, R.A., et al. (2011). MiMIC: a highly versatile transposon insertion resource for engineering Drosophila melanogaster genes. Nat. Methods *8*, 737–743.

Wang, S., Zhao, Y., Leiby, M., and Zhu, J. (2009). A New positive/negative selection scheme for precise BAC recombineering. Mol. Biotechnol. *42*, 110–116.